Computational Uncertainty of Electromagnetic Power Absorption and Temperature Rise in the Eyes Under Exposure to Plane Waves from 1 to 10 GHz

Ilkka Laakso
Department of Radio Science and Engineering, Helsinki University of Technology
Otakaari 5 A, 02150 Espoo, Finland
ilkka.laakso@tkk.fi

***Abstract*— Temperature rise in the eyes caused by exposure to radio-frequency electromagnetic waves is studied. Anatomically realistic male and female head voxel models with three different resolutions, 2 mm, 1 mm, and 0.5 mm, are used. This allows the studies of the uncertainty due to computational resolution, and high resolution allows the frequency range to be increased up to 10 GHz. Plane waves from various directions are used as the exposure source. Electromagnetic power absorption in the head is solved using the finite-difference time-domain (FDTD) method and the thermal model is based on the steady-state bioheat equation, which is solved with finite-difference method using geometric multigrid method for faster convergence.**

The results give empirical rules for sufficient resolution for computing SAR and temperature rise in the eyes, and show differences between open and closed eyes. It is also shown that eye-averaged SAR is a useful measure for the temperature rise in the lens only for frequencies smaller than 3 GHz.

Key words: finite-difference time-domain (FDTD), bioheat, specific absorption rate (SAR), eye temperature

I. Introduction

Exposure to radio-frequency electromagnetic fields may cause risk of permanent biological damage due to overheating in the eyes. Specific absorption rate (SAR) and temperature rise in the eyes have been studied for several different scenarios, including e.g. exposure to normally [1] and obliquely [2] incident plane-waves in the frequency range 0.6 – 6 GHz, and dipole antennas up to 1.9 GHz [3]. The results for electrogeometrical CAD model and anatomically realistic voxel model have been compared in [4] for various sources, including a mobile phone model. Realistic sources have also been studied in [5]. Vascularized eye model for thermal calculation has been used instead of the bioheat equation in [6]. The so-called heat factor of the lens (or eye), i.e., ratio of maximum temperature rise in the lens and eye-averaged SAR (the total electromagnetic power loss in the eye divided by the eye mass) has been discussed in [7], where the heat factor was found to be relatively constant under 3 GHz. Thus eye-averaged SAR might be a good simple measure for the temperature rise in the eye.

In this paper, exposure to plane waves is studied for frequency range up to 10 GHz. SAR and temperature rise for two models with open and closed eyes are compared, and heat factor of the lens is studied. A special focus will be on the uncertainty due to computational resolution, which is studied by calculating the results for three different resolutions.

II. Methods and models

A. Finite-difference time-domain method

The widely-used finite-difference time-domain (FDTD) method [8] was used to solve the absorbed electromagnetic power inside the head tissues. The employed FDTD code has been previously used in [9]. In terminating the computational domain, eight-cell thick convolutional perfectly matched layer (CPML) boundary conditions by [10] were used. The performance of PML for SAR calculations has been tested previously in [11] and [12]. The maximum frequency for FDTD simulations is limited by the resolution of the computational model, as typically the cell size should be smaller than one tenth of the wavelength.

B. Bioheat equation and heat transfer correction

The temperature rise due to the absorption of electromagnetic power was solved by the bioheat equation [13]. In this study, the temperature rise T was solved for the steady-state case, where the time-derivates have been set to zeros, and the equation is of the elliptic form

$$\nabla \cdot (k\nabla T) - BT + S = 0, \tag{1}$$

with boundary condition

$$k\frac{\partial T}{\partial n} + HT = 0, \tag{2}$$

where k is the thermal conductivity, B is related to blood perfusion rate, S is the electromagnetic power-loss density, and H is the heat transfer coefficient between air and tissue. The numerical values of these thermal parameters are presented in Section II-D. The equation was discretized similarly to e.g. [14].

To reduce the overestimation of air-skin boundary area due to the staircase approximation of curved boundaries, conformal heat transfer correction scheme by [14] was used. In this work, this scheme was simplified for easier implementation

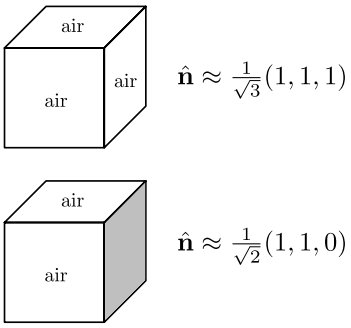

Fig. 1. Approximate normal vector directions for cells with three or two faces on the air-skin boundary

by scaling the heat transfer coefficient H from a skin cell to air to

$$H = \frac{H_0}{\sqrt{N}}, \tag{3}$$

where N is the number of neighboring air cells, and H_0 is the original heat transfer coefficient from skin to air. This simple formula corresponds to the scheme used in [14], with the normal vector determined approximately from the number of neighboring air cells, as illustrated in Fig. 1. No global information of the normal vector is needed, which allows the scheme to be easily applied for voxel models without CAD models available. Using this scheme, the heat transfer to air is decreased, so this gives conservative estimates compared to the uncorrected case.

The discretized equation was solved using geometric multigrid method with Gauss-Seidel iteration. This approach gives the same results as plain Gauss-Seidel (or SOR) iteration, but only with faster convergence. With an ordinary desktop computer, residual norm 10^{-10} could be attained in about 10 minutes for a 0.5 mm resolution head model.

C. Head models

Two head models were employed in this study, namely adult male and female models originating from the Virtual Family project [15]. The models are originally anatomically realistic whole-body CAD models, from which 2 mm, 1 mm and 0.5 mm voxel head models were produced.

In the original models, the eyes are closed. For this study, the eyes were opened by removing the eyelids for studying the differences in absorbed power and temperature rise between open and closed eyes. Masses of the right and left eyes are 6.7 g and 6.8 g for the male model, and 8.4 g and 8.7 g for the female model.

D. Material parameters

Electrical parameters of tissues were those in [16], [17]. Thermal parameters of the main tissues near the eyes are shown in Table I. Due to the limited resolution, sclera, retina and choroid are combined into a single composite tissue, with blood perfusion rate the same as in [7]. The heat transfer coefficients H_0 in (3) for skin and cornea were 8 $\mathrm{W(m^2K)^{-1}}$ and 20 $\mathrm{W(m^2K)^{-1}}$, respectively, as in [7].

TABLE I
THERMAL PARAMETERS OF MAIN TISSUES

Tissue	k $[\mathrm{W(mK)^{-1}}]$	B $[\mathrm{W(m^3K)^{-1}}]$	ρ $[\mathrm{kgm^{-3}}]$
Blood vessel	0.51	716100	1060
Brain grey matter	1.13	47100	1039
Brain white matter	0.50	16700	1043
Cartilage	0.47	3700	1100
Cerebrospinal fluid	0.60	0	1007
Connective tissue	0.37	2700	1013
Eye cornea	0.52	0	1076
Eye lens	0.40	0	1090
Eye sclera/choroid/retina	0.40	80000	1032
Eye humour	0.59	0	1009
Fat	0.25	1700	916
Mucosa	0.34	8500	1050
Muscle	0.53	2000	1041
Nerve	0.46	38500	1038
Skin	0.35	7200	1100
Skull	0.40	3000	1990

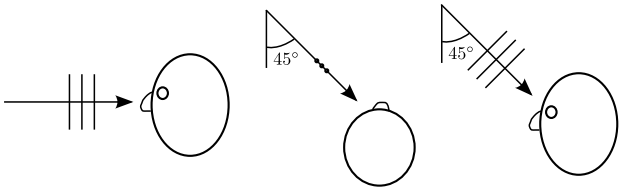

Fig. 2. Incident angles of the plane waves

E. Source plane wave

Power density of the incident plane wave was 10 $\mathrm{Wm^{-2}}$, and it was vertically polarized. The power density corresponds to reference level by ICNIRP [18] or maximum permissible exposure by IEEE [19] for frequencies over 2 GHz for general public exposure (under 2 GHz, the limits decrease linearly to 5 $\mathrm{Wm^{-2}}$ at 1 GHz). Three different incident directions were studied: from the front, from the front left, and from the upfront, as illustrated in Fig. 2.

III. RESULTS

All results are presented as a function of frequency on a semi-logarithmic scale from 1 to 10 GHz. Unless otherwise specified, all presented results are for the resolution of 0.5 mm.

A. SAR and temperature rise in the eyes

Figure 3 shows the eye-averaged SAR for the plane-wave incident from the front left. The respective maximum temperature rise in the lens is shown in Fig. 4. Other incident angles (not plotted) gave somewhat similar results, but the front left direction typically gave the largest SAR for the left eye. For all incident angles and all models, the eye-averaged SAR always stayed under 0.5 $\mathrm{Wkg^{-1}}$. Similarly, the maximum temperature rise in the lens always stayed under 0.1 °C. The eye-averaged SAR seems to decrease with frequency, with a "peak" at around 2 GHz. However, the maximum temperature rise in the lens does not seem to decrease with frequency. Thus the ratio of temperature rise and SAR increases with frequency, as is seen in figure 5, which plots the heat factor of the lens. The heat factor was relatively similar for all incident

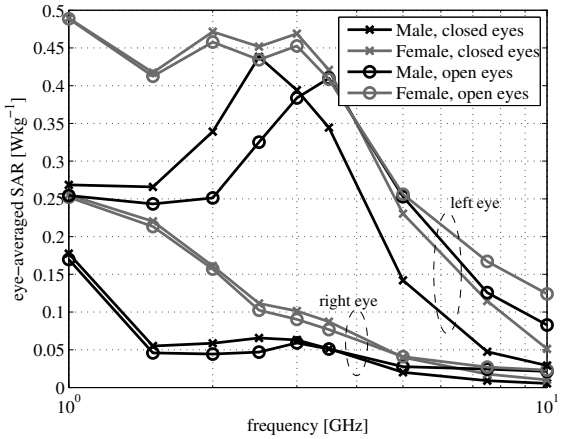

Fig. 3. Eye-averaged SAR for the plane-wave incident from the front left. The upper four curves are for the left eye, and the lower four for the right eye.

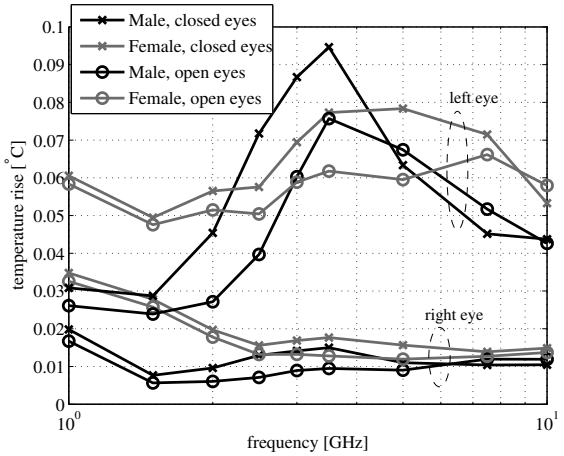

Fig. 4. Maximum temperature rise in the lens for the plane-wave incident from the front left. The upper four curves are for the left eye, and the lower four for the right eye.

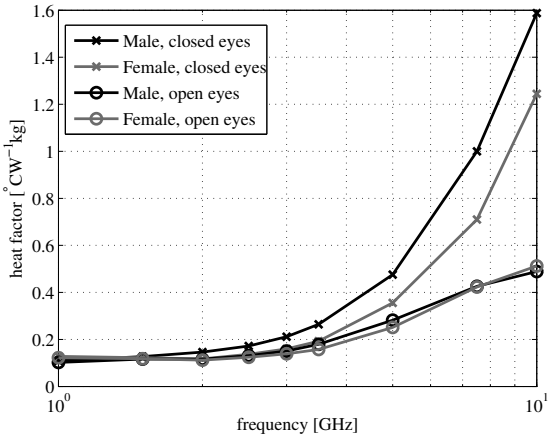

Fig. 5. Heat factor of the lens. For each frequency and model, the values are averaged over left and right eyes and the three incident angles.

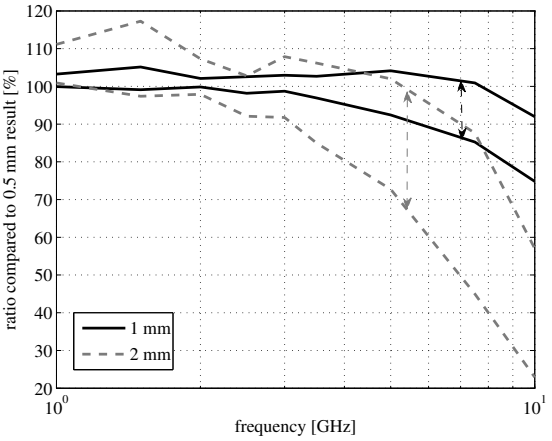

Fig. 6. Range of variation of 2 mm and 1 mm results compared to 0.5 mm results in eye-averaged SAR. 100 % = 0.5 mm result.

angles and both left and right eyes, so the shown heat factor is averaged over these six cases.

The use of heat transfer correction, as described in Section II-B, resulted in 2 to 11 % higher temperatures in the lens than without correction. The difference was larger for open eyes and increased with frequency.

B. Effects of resolution

The uncertainty due to computational resolution was studied by comparing the results calculated with 2 mm and 1 mm resolutions to 0.5 mm resolution results, which were considered the most accurate. Figures 6 and 7 show the ranges of variation for eye-averaged SAR and heat factor of the lens compared to 0.5 mm result, respectively. The range of variation of the lower resolution results compared to the corresponding 0.5 mm results was determined over a total of 24 cases, i.e. over both models, all incident angles, left and right eyes, as well as open and closed eyes. The variation in the maximum temperature rise in the lens was slightly smaller than the variation of eye-averaged SAR, but otherwise very similar.

IV. Discussion and conclusions

Based on the results, it is possible to derive empirical rules of thumb for sufficient resolution for calculation of eye-averaged SAR and temperature rise. By Figs. 6 and 7, it seems that 2 mm resolution might be sufficient for frequencies smaller than 2.5 – 3 GHz, with typical variation from 0.5 mm results less than 10 %. When using 2 mm resolution, the variation in e.g. eye-averaged SAR was relatively large even for low frequencies, which suggests that the variation might be not only due to insufficient resolution for FDTD, but also partly due to insufficient accuracy for anatomical details. Using 1 mm resolution gave much smaller variation than 2 mm resolution. For 1 mm, the maximum frequency seems to be 5 GHz, after which the results start to diverge from the 0.5 mm results. However, the heat factor of the lens might be reasonable even for higher frequencies, even though SAR by

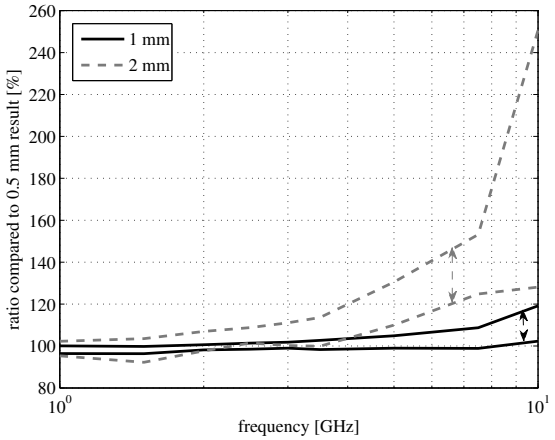

Fig. 7. Range of variation of 2 mm and 1 mm results compared to 0.5 mm results in the heat factor of the lens with respect to the eye-averaged SAR. 100 % = 0.5 mm result.

itself is inaccurate. The effects of resolution have also been studied in [20] for whole-body SAR up to 6 GHz, and the results seem to match well, although the highest frequency for 2 mm resolution seems to be somewhat lower in that study.

In all cases in this study, compliance with reference levels (ICNIRP) or maximum permissible exposure (IEEE) for plane-wave power density implied that the temperature rise in the lens was less than 1 °C, even for occupational exposure. Also, it ensured that eye-averaged SAR stayed under the ICNIRP basic restriction limits.

Eye-averaged SAR has been observed to be a good measure for the maximum temperature rise in the eye [7][5], at least under 3 GHz. Heating factor with respect to eye-averaged SAR rises rapidly with frequency above 3 GHz, as larger fraction of the energy is absorbed in the front of the eye near the lens. As also observed in [7], eye-averaged SAR does not seem to be a good measure for temperature rise for frequencies larger than 3 GHz, because, at high frequencies, even small eye-averaged SAR may cause relatively large heating in the lens. In the new recommendations by IEEE [19], spatially-averaged SAR is only used for frequencies up to 3 GHz, which in this respect seems to be a better choice than to use SAR to up to 10 GHz as in [18] (ICNIRP).

Closed eyes typically gave higher heating factor than open eyes, because heat diffusion into air is smaller due to the insulating eyelids, at least when assuming that the possible thermoregulatory response is ignored. Not only the heat factor, but also the temperature rise was typically larger in closed than in open eyes. Eye-averaged SAR was usually similar in magnitude for both open and closed eyes. From Fig. 5, it seems that, for the heat factor at high frequencies, the difference between open and closed eyes is more important than the differences between different anatomical models.

ACKNOWLEDGEMENTS

Financial support received from GETA (Graduate School in Electronics, Telecommunication and Automation) is acknowledged. Computational resources of CSC (Finnish IT Center for Science) were used in this study.

REFERENCES

[1] A. Hirata, S. Matsuyama, and T. Shiozawa, "Temperature rises in the human eye exposed to EM waves in the frequency range 0.6-6 GHz," *IEEE Trans. Electromagn. Compat.*, vol. 42, no. 4, pp. 386–393, 2000.

[2] A. Hirata, H. Watanabe, and T. Shiozawa, "Sar and temperature increase in the human eye induced by obliquely incident plane waves," *IEEE Trans. Electromagn. Compat.*, vol. 44, no. 4, pp. 592–594, 2002.

[3] A. Hirata, "Temperature increase in human eyes due to near-field and far-field exposures at 900 MHz, 1.5 GHz, and 1.9 GHz," *IEEE Trans. Electromagn. Compat.*, vol. 47, no. 1, pp. 68–76, 2005.

[4] C. Buccella, V. D. Santi, and M. Feliziani, "Prediction of temperature increase in human eyes due to RF sources," *IEEE Trans. Electromagn. Compat.*, vol. 49, no. 4, pp. 825–833, 2007.

[5] P. R. Wainwright, "Computational modelling of temperature rises in the eye in the near field of radiofrequency sources at 380, 900 and 1800 MHz," *Phys. Med. Biol.*, vol. 52, no. 12, pp. 3335–3350, 2007.

[6] V. M. M. Flyckt, B. W. Raaymakers, H. Kroeze, and J. J. W. Lagendijk, "Calculation of SAR and temperature rise in a high-resolution vascularized model of the human eye and orbit when exposed to a dipole antenna at 900, 1500 and 1800 MHz," *Phys. Med. Biol.*, vol. 52, no. 10, pp. 2691–2701, 2007.

[7] A. Hirata, S. Watanabe, O. Fujiwara, M. Kojima, K. Sasaki, and T. Shiozawa, "Temperature elevation in the eye of anatomically based human head models for plane-wave exposures," *Phys. Med. Biol.*, vol. 52, no. 21, pp. 6389–6399, 2007.

[8] A. Taflove and S. C. Hagness, *Computational Electrodynamics: The Finite-Difference Time-Domain Method*, 3rd ed. Boston: Artech House, 2005.

[9] T. M. Uusitupa, S. A. Ilvonen, I. M. Laakso, and K. I. Nikoskinen, "The effect of finite-difference time-domain resolution and power-loss computation method on SAR values in plane-wave exposure of Zubal phantom," *Phys. Med. Biol.*, vol. 53, no. 2, pp. 445–452, 2008.

[10] J. A. Roden and S. D. Gedney, "Convolution PML (CPML): An efficient FDTD implementation of the CFS-PML for arbitrary media," *Microw. Opt. Tech. Lett.*, vol. 27, no. 5, pp. 334–339, 2000.

[11] R. P. Findlay and P. J. Dimbylow, "Variations in calculated SAR with distance to the perfectly matched layer boundary for a human voxel model," *Phys. Med. Biol.*, vol. 51, pp. N411–N415, 2006.

[12] I. Laakso, S. Ilvonen, and T. Uusitupa, "Performance of convolutional PML absorbing boundary conditions in finite-difference time-domain SAR calculations," *Phys. Med. Biol.*, vol. 52, no. 23, pp. 7183–7192, 2007.

[13] H. H. Pennes, "Analysis of tissue and arterial blood temperature in the resting human forearm," *J. Appl. Physiol.*, vol. 1, pp. 93–122, 1948.

[14] E. Neufeld, N. Chavannes, T. Samaras, and N. Kuster, "Novel conformal technique to reduce staircasing artifacts at material boundaries for FDTD modeling of the bioheat equation," *Phys. Med. Biol.*, vol. 52, no. 15, pp. 4371–4381, 2007.

[15] A. Christ, W. Kainz, E. Hahn, K. Honegger, M. Zefferer, E. Neufeld, W. Rascher, R. Janka, W. Bautz, J. Chen, B. Kiefer, P. Schmitt, H. P. Hollenbach, J. X. Shen, M. Oberle, A. Kam, and N. Kuster, "The Virtual Family - Development of anatomical CAD models of two adults and two children for dosimetric simulations," 2008, manuscript in preparation.

[16] S. Gabriel, R. W. Lau, and C. Gabriel, "The dielectric properties of biological tissues: II. measurements in the frequency range 10 Hz to 20 GHz," *Phys. Med. Biol.*, vol. 41, no. 11, pp. 2251–2269, 1996.

[17] ——, "The dielectric properties of biological tissues: III. parametric models for the dielectric spectrum of tissues," *Phys. Med. Biol.*, vol. 41, no. 11, pp. 2271–2293, 1996.

[18] ICNIRP, "Guidelines for limiting exposure to time-varying electric, magnetic and electromagnetic fields (up to 300 GHz)," *Health Phys.*, vol. 74, pp. 492–522, 1998.

[19] IEEE, *IEEE Standard for Safety Levels with Respect to Human Exposure to Radio Frequency Electromagnetic Fields, 3 kHz to 300 GHz, C95.1-2005*. New York: Institute of Electrical and Electronics Engineers, 2005.

[20] P. Dimbylow and W. Bolch, "Whole-body-averaged SAR from 50 MHz to 4 GHz in the University of Florida child voxel phantoms," *Phys. Med. Biol.*, vol. 52, no. 22, pp. 6639–6649, 2007.